Second Harmonic Generation due to Quadrupole Interaction in a Photonic Crystal Slab: Angle Dependence and Symmetry of the Unit Cell

Teruya Ishihara* and Kazuki Koshino
Frontier Research System, RIKEN, 2-1 Hirosawa, Wako 351-0198, Japan

Hisashi Nakashima†
Graduate School of Advanced Sciences of Matter, Hiroshima University, Higashi-Hiroshima 739-8530, Japan
(Received 28 February 2003; published 16 December 2003)

We investigate second harmonic generation (SHG) from a photonic crystal slab consisting of centrosymmetric materials. The SHG signal is observed in the transmission direction when the incident laser excites the quasiwaveguide mode. As the SHG frequency approaches the exciton level, the SHG intensity increases resonantly. When the incident angle is exactly 0, the SHG signal vanishes even if the transmission dip is excited. This fact is readily explained by a quadrupole theory based on the Lorentz oscillator model, where the source of the nonlinearity is the Lorentz force. When the unit cell in the photonic crystal lacks inversion symmetry, the SHG signal is expected even for the normal incidence. It is experimentally demonstrated for a square array of triangular semiconductor slabs.

DOI: 10.1103/PhysRevLett.91.253901 PACS numbers: 42.70.Qs, 42.55.Tv, 42.65.Ky, 71.35.Cc

The photonic crystal is a periodic structure of materials on the optical wavelength scale. This concept was introduced as a tool to inhibit spontaneous emission in semiconductors [1]. Even though it does not yield a complete band gap, such a periodic structure may provide a unique physical environment, where electromagnetic mode symmetry is very different from that of plane waves in free space. The lattice symmetry effect on electromagnetic field distribution in 2D photonic crystal slabs was investigated in [2,3]. The effect of the asymmetric unit cell was demonstrated as well for a photonic crystal slab with obliquely deposited organic molecules [4]. The transmission and emission spectra were found to be asymmetric in respect to the change in sign of the incident angle. Such an asymmetric response naturally triggers an investigation of second order optical nonlinearity.

A second order optical nonlinearity is the lowest nonlinearity and therefore could be the largest. In conventional bulk materials, however, it vanishes if they have center of inversion symmetry under the dipole approximation [5]. Nonlinearity derived from the next higher (quadrupole) approximation shows up in the region where the field is inhomogeneous as in the interface [6]. Recently Feigel *et al.* [7] theoretically studied second order optical nonlinearity due to quadrupole interaction in photonic crystals. They concluded that by tailoring the structure properly, nonlinearity may compete with that resulting from a conventional dipole interaction. Preceding their work, Lamprecht *et al.* [8] demonstrated that the symmetric arrangement of asymmetrical metal nanoparticles in the optical scale results in cancellation of the second harmonic generation (SHG) signal, although the system was not treated as photonic crystals. Martorell *et al.* [9] have investigated three-dimensional photonic crystals consisting of dye-coated polystyrene spheres and found phase matched SHG in the Bragg reflection direction.

In this Letter we report the demonstration of SHG from a photonic crystal slab (PCS) consisting of centrosymmetric materials, and investigate the role of symmetry in quadrupole interaction. For this purpose we have adopted the transmission configuration, which allows the investigation of symmetry at the Γ point in the Brillouin zone. As opposed to the reflected SHG configuration, measurement is more straightforward and therefore reliable because the detector position is fixed. Instead of using plasmon resonance [8], we utilize the exciton level, which is much less structure sensitive, allowing us to obviate the inhomogeneous broadening problem. As is different from Martorell's work, phase matching does not play a role in our thin film configuration.

The structure of our one-dimensional PCS sample is shown schematically in the inset of Fig. 1. A one-dimensional grating structure with a rectangular cross section was engraved on a quartz substrate using electron beam lithography. Gratings (pitch Λ ranging between 670 and 720 nm, the depth 460 nm, groove width $a = 3\Lambda/4$, and area 1.5×1.5 mm^2) were engraved on a quartz substrate. In order to enhance contrast in the dielectric constant a centrosymmetric semiconductor $(C_6H_5C_2H_4NH_3)_2PbI_4$ (PEPI) was embedded in grating grooves by spin coating its acetonitrile solution. The thickness of PEPI at the bottom was estimated to be 40 nm. PEPI crystallizes into self-organized multiquantum wells of PbI layers sandwiched between organic barrier layers. By virtue of the small dielectric constant of the barrier layer, the excitonic binding energy amounts to 220 meV for this compound [10]. Therefore excitonic absorption is clearly seen even at room temperature. The

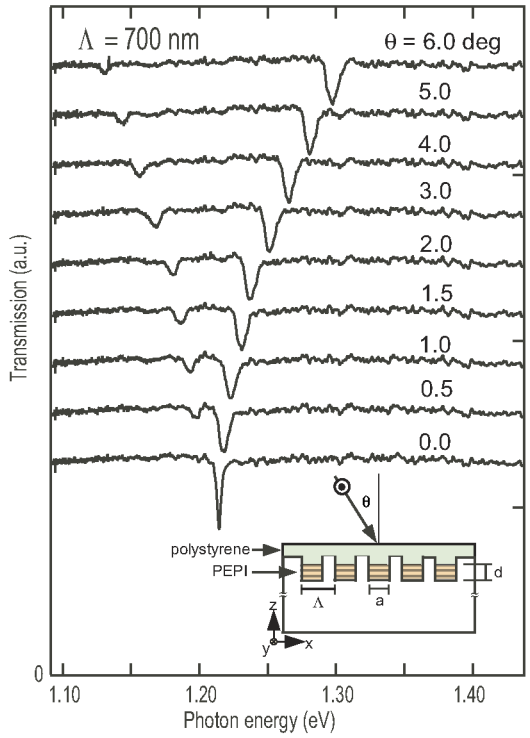

FIG. 1 (color online). Schematic sample structure (inset) and angle dependent transmission spectra for a $\Lambda = 700$ nm sample.

top was given a polystyrene overcoating in order to support guided modes in the sample. Waveguide modes which would exist in a polystyrene/PEPI/quartz plain slab waveguide become leaky due to the periodicity of the PCS. With the help of a reciprocal lattice vector, they can be excited by light coming from the free space. Such excitation appears as narrow dips in transmission spectra.

Figure 1 shows the transmission spectrum in the near infrared region, which corresponds to the first band gap region at the Γ point for this period (700 nm). Two dips seen in each spectrum are ascribed to the excitation of the waveguide modes aided by $+G = 2\pi/\Lambda$ and $-G$ reciprocal lattice vectors, respectively. As θ tends to zero, the two dips draw closer. At normal incidence the lower dip loses its oscillator strength because of its symmetry. The one of the two edges that is active depends on the line-and-space ratio. The energy region between the active upper dip and the extrapolated position of the lower dip is the photonic band gap. The next band gap at the Γ point is located near the exciton resonance at 2.4 eV. Strong coupling between the exciton and the quasiguided wave has been investigated in such structures [11]. For such PCS, we have carried out SHG measurement.

The polarization of the incident light was parallel to the grooves (S polarization). A collimated beam from a tunable pulse laser (optical parametric oscillator, pulse duration 5 ns, repetition 10 Hz) was introduced from the free space to the PCS. By tilting the sample, for each incident photon energy one can generally find the angle

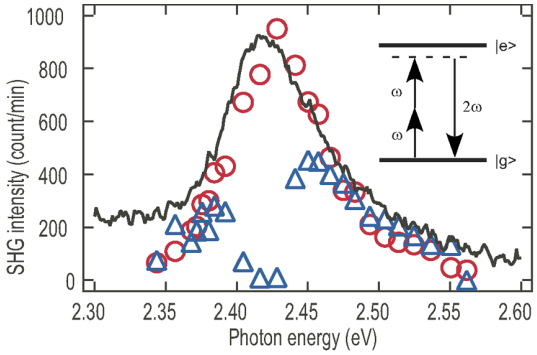

FIG. 2 (color online). SHG intensity as a function of SHG energy for $\Lambda = 650$ nm (○) and 700 nm (△). The solid curve is the absorption spectrum of PEPI film.

for which the guided light comes out from the edge of the sample. At the same time, one can see scattered green light from the grating area. The fundamental frequency is blocked by a band pass filter ($CuSO_4$ aqueous solution).

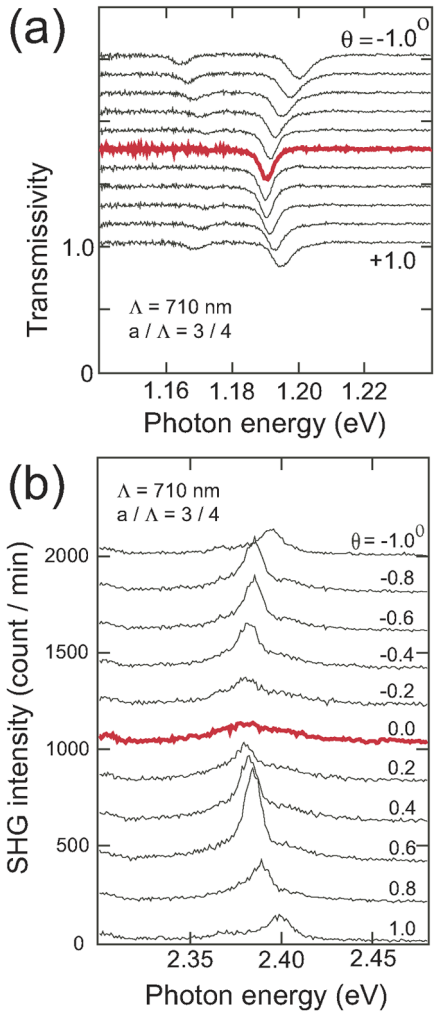

FIG. 3 (color online). (a) Transmission spectra near normal incidence and (b) corresponding SHG excitation spectra for a sample with $\Lambda = 710$ nm.

The signal was observed in the direction of the transmitted light and spectrally dispersed with a charge coupled device polychromator. We found that the signal is monochromatic and exactly at $2\hbar\omega$, where $\hbar\omega$ is the photon energy of the incident laser. We also confirmed that the signal intensity is proportional to the square of the incident laser power. Thus we conclude that the signal is SHG from the PCS consisting of centrosymmetric materials.

The SHG intensity is plotted as a function of SHG photon energy with circular ($\Lambda = 650$ nm) and trianglular ($\Lambda = 700$ nm) marks in Fig. 2. The solid curve in the figure represents the absorption spectrum of a PEPI film. In the case of $\Lambda = 650$ nm, SHG intensity increases as its frequency approaches the exciton level. The enhancement is attributed to the intermediate state resonance in the second harmonic generation process (see the inset). On the other hand, in the case of $\Lambda = 700$ nm, there is a spectral region where no SHG is observed for any $\theta \sim 0$. For this period the exciton resonance falls into the photonic band gap where the quasiwaveguide mode is not excited. SHG conversion efficiency was estimated to be 10^{-14} for the pump intensity of 1 MW/cm^2. This conversion efficiency was comparable to that of the reflected SHG from a GaAs bulk crystal, which lacks inversion symmetry.

In order to investigate the role of symmetry, we have examined the optical resonance near normal incidence. Figure 3(a) shows the transmission spectra for near normal incident angles between $+1.0°$ and $-1.0°$. Generally two dips are observed in finite incident angles. At $\theta = 0$, however, only a higher energy mode is seen in the transmission spectra, which reflects the symmetries at the Γ point. Figure 3(b) shows the SHG excitation spectra for the same incident angles. Generally when the incident light matches the dip in the transmission spectrum, SHG is observed. It is clearly seen, however, that the SHG intensity vanishes for normal incidence. The same tendency was observed in any symmetric gratings we investigated. SHG from the lower photonic band cannot be seen in these particular data due to the small coupling to the band and weak incident beam intensity, used to avoid degradation during measurement. If the incident light intensity were larger, it would have been apparent.

Next we introduce an isotropic Lorentz oscillator model in order to explain SHG from the centrosymmetric material. The equation of motion for an electron is given by

$$m(\ddot{\boldsymbol{r}} + \omega_0^2 \boldsymbol{r}) = \sqrt{f} e[\boldsymbol{E}(\boldsymbol{r}, t) + \dot{\boldsymbol{r}} \times \boldsymbol{B}(\boldsymbol{r}, t)],$$

where m is the electron mass, $\hbar\omega_0$ the exciton energy, e the electron charge, and f the exciton oscillator strength. Because of the Lorentz magnetic force, the electron follows a curved trajectory, which is the origin of nonlinearity. To second order of the field amplitude, nonlinear polarization at the semiconductor layer is expressed as

$$\boldsymbol{P}_\omega = \epsilon_0 \chi(\omega) \boldsymbol{E}_\omega, \qquad \boldsymbol{P}_{2\omega} = \frac{\epsilon_0^2}{\rho e} \chi(\omega)\chi(2\omega)\Xi(x, z)[(\boldsymbol{E}_\omega \cdot \boldsymbol{\nabla})\boldsymbol{E}_\omega + \boldsymbol{E}_\omega \times (\boldsymbol{\nabla} \times \boldsymbol{E}_\omega)],$$

$$\chi(\omega) = \frac{\sqrt{f}\rho e^2}{m\epsilon_0(\omega_0^2 - \omega^2)} = \frac{\sqrt{f}\omega_p^2}{(\omega_0^2 - \omega^2)},$$

where ω is the light frequency, ρ the oscillator density, $\chi(\omega)$ the linear susceptibility, and $\omega_p = [\rho e^2/\epsilon_0 m]^{1/2}$ the plasma frequency. For $\chi(2\omega)$, the denominator vanishes as SHG frequency approaches the exciton level, when an implicit imaginary part should be taken into account. This resonance is responsible for the experimentally observed frequency dependence. $\Xi(x, z) = X(x)Z(z)$ is a function which describes spatial distribution of the periodically arranged semiconductor strips: $Z(z) = 1$ for $|z| < d/2$ and otherwise vanishes, where d is the PEPI thickness. $X(x)$ is a periodic function, $X(x + \Lambda) = X(x)$, and is unity for $|x| < a/2$, while it vanishes for $a/2 < |x| < \Lambda/2$. Because of the periodicity, $X(x)$ can be expanded in terms of the reciprocal lattice vector G: $X(x) = \sum \xi_{nG} e^{inGx}$. Note that ξ_{nG} is the parameter which can be controlled by the lithography design.

When the S-polarized incident field $(0, E_0 e^{ipx+iqz}, 0)$ matches the waveguide mode by choosing the appropriate incident angle, the strong electromagnetic field is excited in the waveguide mode. The electric field that appeared in the expression for $\boldsymbol{P}_{2\omega}$ can be replaced by the waveguide field E_g because it is much larger than the radiation modes, and $E_g(x) = E_0[R_+ e^{i(p+G)x} + R_- e^{i(p-G)x}]$ where R_+ and R_- depend on the PCS parameters and are functions of p and ω. The derivation of R_+ and R_- will be published elsewhere [12]. Note that for our experimental configuration (S polarization and $d/dy = 0$), the first term of $\boldsymbol{P}_{2\omega}$ in the square brackets vanishes. Because this second order nonlinear polarization includes spatial derivatives, it is classified as the quadrupole effect.

From $I_{\mathrm{SHG}} = (c/2\mu_0)[i\mu_0\omega \int dz P_{2\omega}]^2$, the SHG efficiency in our model is given by $I_{\mathrm{SHG}}/I_0 = Ag(\omega)h(p, \omega)$, where

$$A = \left[\frac{eE_0}{cm\omega}\right]^2, \qquad g(\omega) = [\chi(\omega)\chi(2\omega)]^2 f, \qquad h(p, \omega) = d^2[(p + G)\xi_{-2G}R_+^2 + 2p\xi_0 R_+ R_- + (p - G)\xi_{2G}R_-^2]^2,$$

are the intrinsic, material, and structure factors, respectively. Since $R_+ = R_-$ for $p = 0$(normal incidence), $\boldsymbol{P}_{2\omega}$ vanishes as long as $\xi_{2G} = \xi_{-2G}$, which holds for our symmetric grating structure (symmetric with respect to x).

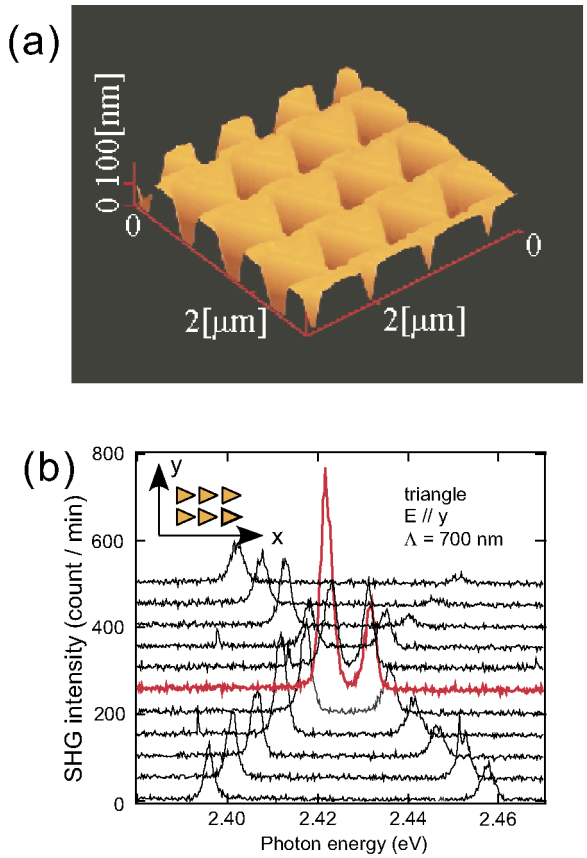

FIG. 4 (color online). (a) Atomic force microscope image of the patterned substrate. (b) SHG excitation spectra for the two-dimensional triangular arrays.

To demonstrate that the design of the photonic crystal readily brings about changes in nonlinear optical properties, we have carried out the same experiment using an asymmetrically patterned substrate. Figure 4 shows the atomic force microscope image of the sample we used. Equilateral triangles with a height of 600 nm and a base of 500 nm were arranged on a square lattice with a pitch of 700 nm. The sample filled with PEPI and overcoated with polystyrene was set so that the symmetry was broken in the x direction. Polarization of the incident laser beam was parallel to the triangular base.

For a given incident angle, when the incident frequency matches that of the waveguide mode, SHG is generated in the transmission direction as in the simple grating sample. Polarization of SHG was perpendicular to that of the incident beam. As the incident angle approaches 0, SHG intensity from the upper band increases which shows prominent contrast from the case of rectangular gratings. In the context of our theory, this can be understood in terms of $\xi_{2G} \neq \xi_{-2G}$, because of the broken symmetry at the Γ point. Note that SHG from the lower band is also observed near normal incidence. In this case the broken symmetry acts to recover the transmission dips for the normal incidence as well.

In this study we have demonstrated that SHG is sensitive to the symmetry of the PCS as well as the geometry. We did not particularly intend to optimize conversion efficiency. In order to apply this mechanism to practical application, one should consider a multilayer structure with phase matching. In the PCS of centrosymmetric materials, the quadrupole effect can readily contribute to the second order nonlinear process when symmetry is broken. Thus the majority of materials with inversion symmetry are now qualified as second order nonlinear optical materials.

The authors acknowledge Professor G. Mizutani and Dr. N. A. Gippius for their valuable comments.

*Electronic address: terish@postman.riken.go.jp
†Present address: Kyocera, Kyoto 612-8501, Japan.

[1] E. Yablonovitch, Phys. Rev. Lett. **58**, 2059 (1987).
[2] T. Ochiai and K. Sakoda, Phys. Rev. B **64**, 045108 (2001).
[3] S. G. Tikhodeev, A. L. Yablonskii, E. A. Muljarov, N. A. Gippius, and T. Ishihara, Phys. Rev. B **66**, 045102 (2002).
[4] T. Fujita, T. Kitabayashi, A. Seki, M. Hirasawa, and T. Ishihara, Physica (Amsterdam) **7E**, 681 (2000).
[5] Y. R. Shen, *The Principles of Nonlinear Optics* (John Wiley & Sons, New York, 1984).
[6] N. Bloembergen and P. S. Pershan, Phys. Rev. **128**, 606 (1962).
[7] A. Feigel, Z. Kotler, and B. Sfez, Phys. Rev. B **65**, 073105 (2002).
[8] B. Lamprecht, A. Leitner, and F. R. Aussenegg, Appl. Phys. B **68**, 419 (1999).
[9] J. Martorell, R. Vilaseca, and R. Corbalan, Appl. Phys. Lett. **70**, 702 (1997); Phys. Rev. A **55**, 4520 (1997); J. Trull, J. Martorell, and R. Vilaseca, J. Opt. Soc. Am. B **15**, 2581 (1998).
[10] T. Ishihara, *Optical Properties of Low-Dimensional Materials*, edited by T. Ogawa and Y. Kanemitsu (World Scientific, Singapore, 1995), Chap. 6, pp. 289–339.
[11] T. Fujita, Y. Sato, T. Kuitani, and T. Ishihara, Phys. Rev. B **57**, 12 428 (1998).
[12] K. Koshino, Phys. Rev. B **67**, 165213 (2003).